

## Performance Analysis of Low-power Tokamak Reactors

G.O. Ludwig 1), M.C.R. Andrade 1), M. Gryaznevich 2), T.N. Todd 2)

1) Laboratório Associado de Plasma, INPE, São José dos Campos, SP, Brazil

2) EURATOM/UKAEA Fusion Association, Culham Science Center, Abingdon, UK

e-mail contact of main author: [ludwig@plasma.inpe.br](mailto:ludwig@plasma.inpe.br)

**Abstract.** Global models are useful in the analysis of fusion reactors due to the facility in computing and presenting the results in terms of comprehensive parameters. A general figure of merit, which encompasses all the relevant tokamak parameters, is introduced in this article by a convenient normalization of the global power balance equation. In this way, different hypothetical tokamak reactors can be compared in terms of their figure-of-merit value. This criterion is applied to analyze the performance of both ITER-like reactors and a class of newly proposed low-power reactors.

### 1. Introduction

A new approach to fusion power has been recently considered – to demonstrate early power production in a compact reactor with low first wall load [1,2]. The reduced load allows using presently available first wall technologies, until new materials are developed and tested by ITER and future component-testing facilities. However, the use of the small fusion power output of the pilot plant has to be optimized either by energy multiplication methods (fuel breeding) or in applications such as high-level waste transmutation, hydrogen production at high temperature, and testing of fusion nuclear technology components [3,4,5,6]. Low-aspect-ratio tokamaks with increased toroidal field seem to be the ideal candidates for these applications, either by using replaceable central copper rods [5,6] or perhaps high temperature superconductor technology [7,8,9]. In this context the fusion hybrid is not a new idea, it was strongly advocated by Hans Bethe in the 70's [10], but gets a new perspective when applied to low-power tokamaks using the advantages of spherical configurations.

In this article the performance of low-power tokamak reactors is analyzed, considering the fusion power, fusion gain and average wall load. The analysis is based on a simple global model with the conduction and convection losses modeled by empirical scaling laws (ITER IPB98 scaling law in particular). The plasma model includes geometrical aspects, profiles and impurities effects, neoclassical effects, and stability constraints. Stability issues related to the toroidal beta limit, safety factor and density limit are taken into account. Then, a convenient normalization of the plasma temperature and density, and of the auxiliary power, is introduced, which leads to the definition of a figure-of-merit parameter [11]. This figure of merit defines the performance of tokamak reactors in a simple way. Its use allows to search for sets of machine parameters that satisfy the performance goal, and to classify different tokamaks by their figure-of-merit value.

The article is organized as follows. Section 2 briefly presents the plasma model and the formulas used to evaluate the total power associated with radiation loss, alpha particles heating, and ohmic power heating, respectively. These formulas are well known and discussed, for example, in the Wesson book [12]. They constitute the POPCON model developed by many authors in the 80's [13], and are presented for completeness and uniformity in the notation. In Section 3 the power balance equation is normalized and the figure-of-merit criterion is introduced. Section 4 illustrates the application of the figure of merit approach both to describe an ITER-like reactor and to analyze the performance of low-power tokamak reactors according to the above introductory definition.

## 2. Plasma model and power balance

The area of the poloidal cross-section  $A_p$  and the plasma volume  $V_p$  are given, to order  $\delta^2$ , respectively by

$$A_p = \pi \kappa a^2 (1 - \delta^2/4) \text{ and } V_p = 2\pi^2 \kappa R_0 a^2 [1 - a\delta/(4R_0) - \delta^2/4],$$

where  $R_0$  is the geometrical major radius and  $a$  is the minor radius of the plasma poloidal cross-section,  $\kappa$  is the elongation, and  $\delta$  is the triangularity. Neglecting triangularity corrections, the plasma surface is approximately given by

$$A_s \approx 4\pi^2 a R_0 [(1 + \kappa^2)/2]^{1/2}$$

to within 5% for  $1 \leq \kappa \leq 3$ . This formula is useful for estimating the wall loading on a close wall.

The radial profiles of the particle density, temperature and current density are given by the usual binomial expressions:  $n(r) = (1 + \alpha_n) \langle n \rangle (1 - r^2/a_p^2)^{\alpha_n}$ ,

$$T(r) = (1 + \alpha_n + \alpha_T) (1 + \alpha_n)^{-1} \langle T \rangle (1 - r^2/a_p^2)^{\alpha_T} \text{ and } j_p(r) = (1 + \alpha_j) \langle j_p \rangle (1 - r^2/a_p^2)^{\alpha_j},$$

where  $\langle n \rangle = \langle n_e + n_i \rangle / 2$ ,  $\langle T \rangle = \langle n_e T_e + n_i T_i \rangle / \langle n_e + n_i \rangle$  and  $\langle j_p \rangle = I_p / A_p$  are the volume average particle density, density-averaged temperature and average current density;  $\alpha_n$ ,  $\alpha_T$  and  $\alpha_j$  are the profile peaking factors; and  $a_p = (A_p / \pi)^{1/2}$  is the equivalent minor radius of the plasma poloidal cross-section. The cylindrical safety factor  $q_*$  is defined in terms of both the toroidal induction  $B_0$  at the major radius  $R_0$  and the average plasma current density  $\langle j_p \rangle$  by

$$q_* = [2B_0 / (\mu_0 R_0 \langle j_p \rangle)] (1 + \kappa^2) / (2\kappa),$$

and the safety factor on the magnetic axis is approximately given by  $q_0 \approx q_* / (1 + \alpha_j)$ .

The toroidal beta is defined in terms of the total thermal energy of the plasma  $W = 4.81 \times 10^4 \langle n \rangle \langle T \rangle V_p = \langle p \rangle V_p$  and the vacuum toroidal field  $B_0$

$$\beta_T = (W / V_p) / [B_0^2 / (2\mu_0)],$$

while the plasma beta is defined in terms of the ratio between the average plasma pressure  $\langle p \rangle$  and the volume averaged magnetic pressure

$$\beta = \langle p \rangle / [\langle B^2 \rangle / (2\mu_0)].$$

The coefficient in the expression of the thermal energy is such that  $n$  and  $T$  are given in units of  $10^{20} \text{ m}^{-3}$  and keV, respectively. These units will be used throughout this article. In general, the maximum beta for stability is given in terms of the normalized  $\beta_N$  value

$$\beta \leq \beta_N [10^{-6} I_p / (a B_0)] = \beta_N [10^{-6} A_p / (\mu_0 a^2)] [(1 + \kappa^2) / \kappa] \varepsilon / q_* = 5\beta_N [(1 + \kappa^2) / 2] (1 - \delta^2/4) \varepsilon / q_*,$$

where  $\varepsilon = a / R_0$  is the inverse aspect ratio. In the large aspect ratio limit  $\varepsilon \rightarrow 0$  the magnetic field energy is dominated by the vacuum component and  $\beta_N$  coincides with the Troyon factor

$$g_T = \beta_T / [10^{-6} I_p / (a B_0)] < 0.028 \text{ m} \times \text{T/MA}.$$

For ideal no-wall stability  $\beta_N$  is independent of aspect ratio and elongation (the variation on triangularity is within error bars) and takes an approximately constant value  $\beta_N \approx 0.03 \text{ m} \times \text{T/MA}$  for  $q_* > 2$  and  $q_0 > 1$ . Nevertheless,  $\beta_N$  strongly depends on the safety factor profile and recent experimental results demonstrated  $\beta_N \approx 0.057 \text{ m} \times \text{T/MA}$ , above the no-wall ideal-stability limit, by operating with shape and resistive wall mode controls. At last, the Greenwald limit, both in  $10^{20} \text{ m}^{-3}$  and MA/m<sup>2</sup> is

$$n_G \sim j_G = 10^{-6} I_p / (\pi a^2).$$

The irreducible loss in the high-density, low-temperature regime is the total Bremsstrahlung power loss given, in W, by

$$P_r = 5.35 \times 10^3 g_r Z_{\text{eff}} \langle n_e \rangle^2 \langle T_e \rangle^{1/2} V_p,$$

where  $g_r = (1 + \alpha_n)^{3/2} (1 + \alpha_n + \alpha_T)^{1/2} (1 + 2\alpha_n + \alpha_T/2)^{-1}$  is the radiation power profile factor and  $Z_{\text{eff}}$  is the effective ion charge.

The total power deposited by alpha particles is given by

$$P_\alpha = 1.43 \times 10^{27} [4f_D(1-f_D)f_{DT}^2 f_a] g_\alpha (\langle T_i \rangle) \langle n_e \rangle^2 \langle \sigma v \rangle (\langle T_i \rangle) V_p,$$

where  $f_D = \langle n_D \rangle / \langle n_D + n_T \rangle$  is the homogeneous deuterium fraction in the D-T mixture (the optimal value is  $f_D = 0.5$ ),  $f_{DT} = \langle n_D + n_T \rangle / \langle n_e \rangle$  is the dilution factor,  $f_\alpha$  is the alpha-particle containment fraction,  $g_\alpha$  is the alpha particle profile factor and  $\langle \sigma v \rangle$  is the Maxwellian reactivity for the D-T reaction. Assuming an average charge state  $Z$  for the impurities, the condition of quasi-neutrality gives

$$Z_{eff} = Z - (Z-1)f_{DT} - 2(Z-2)\langle n_\alpha \rangle / \langle n_e \rangle \text{ and}$$

$$\langle n \rangle = [1 + f_{DT} + \langle n_\alpha \rangle / \langle n_e \rangle + (1 - f_{DT} - 2\langle n_\alpha \rangle / \langle n_e \rangle) / Z] \langle n_e \rangle / 2,$$

where  $\langle n_\alpha \rangle / \langle n_e \rangle$  is the fraction of alpha particles. If  $f_{DT} \approx 1$  and  $\langle n_\alpha \rangle / \langle n_e \rangle \ll 1$ , one has  $Z_{eff} \approx 1$  and  $\langle n \rangle \approx \langle n_e \rangle$ .

In general, the reactivity must be calculated by integration over the reaction cross-section. However, over limited temperature ranges it is possible to use simple monomial approximations  $\langle \sigma v \rangle (T) \approx C_\alpha T^\alpha$  in  $\text{m}^3/\text{s}$  to within 10% for the reaction rate

$$\begin{aligned} C_\alpha &= 2.2 \times 10^{-26} & \alpha &= 4 & 2.2 \text{ keV} < T < 5.9 \text{ keV} \\ C_\alpha &= 1.1 \times 10^{-25} & \alpha &= 3 & 4.4 \text{ keV} < T < 12.2 \text{ keV} \\ C_\alpha &= 1.1 \times 10^{-24} & \alpha &= 2 & 8.3 \text{ keV} < T < 22.3 \text{ keV} \end{aligned}$$

Using these monomial forms the alpha heating profile factor is temperature independent

$$g_\alpha = (1 + \alpha_n)^2 (1 + 2\alpha_n + \alpha\alpha_T)^{-1} [(1 + \alpha_n + \alpha_T) / (1 + \alpha_n)]^\alpha,$$

and the total power deposited by alpha particles is estimated by

$$P_\alpha \approx 1.43 \times 10^{27} C_\alpha [4f_D(1-f_D)f_{DT}^2 f_\alpha] g_\alpha \langle n_e \rangle^2 \langle T_i \rangle^\alpha V_p.$$

The containment of alpha particles is a topic that deserves special attention, particularly in the case of the low-power configurations considered in this article. Considering first-orbit losses, the alpha particles will be effectively contained, that is  $f_\alpha \approx 1$ , if  $I_p \geq 5.44 \varepsilon^{1/2} (1 + \kappa^2) / (2\kappa)$  MA.

The total ohmic heating power is

$$P_\Omega = 9.61 \times 10^{-10} \ln \Lambda_{ei} Z_{eff} [(2.31 + Z_{eff}) / (0.923 + Z_{eff})] g_\Omega g_{NC} \langle j_p \rangle^2 \langle T_e \rangle^{-3/2} V_p,$$

where the ohmic power profile factor is

$$g_\Omega = (1 + \alpha_j)^2 (1 + 2\alpha_j - 3\alpha_T / 2)^{-1} [(1 + \alpha_n) / (1 + \alpha_n + \alpha_T)]^{3/2},$$

and the neoclassical resistivity enhancement factor is given in the low-collisionality limit by

$$g_{NC} \approx (1 + 2\alpha_j - 3\alpha_T / 2) \int_0^1 x^{2\alpha_j - 3\alpha_T / 2} [1 - f_T(x)]^{-1} [1 - C_Z f_T(x)]^{-1} dx,$$

where  $C_Z = 0.56 [(3 - Z_{eff}) / (3 + Z_{eff})] / Z_{eff}$  and the fraction of trapped particles is

$$f_T(x) = 1 - [1 - \varepsilon(1-x)^{1/2}]^2 [1 - \varepsilon^2(1-x)]^{-1/2} [1 + 1.46 \varepsilon^{1/2} (1-x)^{1/4}]^{-1}.$$

The low-electron-collisionality limit is, in general, a good approximation in the reactor regime, though overestimating the small contribution of ohmic heating to the power balance.

To compensate one takes  $\ln \Lambda_{ei} \approx 17$ . Furthermore, to simplify the calculations it is assumed that  $\langle n_e \rangle \approx \langle n_i \rangle \approx \langle n \rangle$  and  $\langle T_e \rangle \approx \langle T_i \rangle \approx \langle T \rangle$ .

The global power balance is described by the equation

$$\partial W / \partial t = -W / \tau_E + P,$$

where  $W = 4.81 \times 10^4 \langle n \rangle \langle T \rangle V_p$  is the thermal plasma energy defined previously, and the convection and conduction power losses  $P_c = W / \tau_E$  are given in terms of the energy confinement time  $\tau_E$ . The net heating power in this equation is

$$P = P_\alpha + P_\Omega + P_{aux} - P_r,$$

where  $P_\alpha$ ,  $P_\Omega$  and  $P_{aux}$  are the alpha, ohmic and auxiliary input powers, respectively, and  $P_r$  is the radiation power loss. The auxiliary power distribution depends on the type of heating power source. Here, the total auxiliary power is a variable to be determined.

### 3. Normalized power balance equation and the figure of merit

A reference temperature  $\langle T_0 \rangle$ , which is independent of the density and corresponds to the threshold between alpha heating and radiation cooling, is defined by the solution of

$$P_\alpha(\langle n \rangle, \langle T_0 \rangle) = P_r(\langle n \rangle, \langle T_0 \rangle).$$

Using the monomial approximation  $\langle\sigma v\rangle(T)\approx C_\alpha T^\alpha$  with  $3<\alpha<4$ , a simple estimate for the threshold temperature in keV is obtained

$$\langle T_0\rangle\approx\{3.75\times 10^{-24}Z_{\text{eff}}g_r[C_\alpha 4f_D(1-f_D)f_{DT}^2f_\alpha g_\alpha]^{-1}\}^{2/(2\alpha-1)}.$$

This estimate is used as a start value to calculate  $\langle T_0\rangle$  using a precise formula of the reactivity. Nevertheless, a quite good estimate is obtained simply taking the average value of  $\langle T_0\rangle$  obtained with  $3<\alpha<4$ .

Next, a reference density  $\langle n_0\rangle$ , corresponding to the Murakami-Hugill density limit, is defined by the solution of the equation

$$P_r(\langle n_0\rangle, \langle T_0\rangle)=P_\Omega(\langle T_0\rangle),$$

where, in general, the ohmic term is weakly dependent on the density through the Coulomb logarithm and the electron collisionality. Assuming constant Coulomb logarithm and neglecting the effect of collisions in the neoclassical resistivity enhancement factor, the reference density is given in  $10^{20}\text{ m}^{-3}$  simply by

$$\langle n_0\rangle\approx 4.24\times 10^7 [(2.31+Z_{\text{eff}})(0.923+Z_{\text{eff}})^{-1}\ln A_{ei}(g_\Omega g_{NC}/g_r)]^{1/2}\langle j_p\rangle/\langle T_0\rangle.$$

Finally, a dimensionless figure of merit, which is independent of  $P_{\text{aux}}$ , is defined by

$$X=P_r^{1+\gamma_P}(\langle n_0\rangle, \langle T_0\rangle)P_c^{-1}(\langle n_0\rangle, \langle T_0\rangle)P^{\gamma_P}(\langle n_0\rangle, \langle T_0\rangle),$$

where  $\gamma_P$  is the exponent of the net heating power in the scaling law, which is assumed to be of the general form

$$\tau_E\sim C_E H(10^{-6}I_p)^{\gamma_I} B_0^{\gamma_B} (10^{-6}P)^{\gamma_P} A_i^{\gamma_A} \langle n\rangle^{\gamma_n} \langle T\rangle^{\gamma_T} R_0^{\gamma_R} \varepsilon^{\gamma_\varepsilon} \kappa^{\gamma_\kappa}.$$

In this scaling  $H$  is the H-mode enhancement factor and  $A_i=2.5$  is the average atomic mass number for a 50:50 D-T mixture. Observe that this scaling law presents an explicit dependence on the temperature  $\langle T\rangle$ . In general, the temperature is implicit in the net heating power dependence. In this article the dependence on  $\langle T\rangle$  is maintained only to demonstrate the compatibility of the model with older scaling laws, prior to the introduction of the explicit dependence on the heating power. For the ITER IPB98(y,2) scaling, in particular,

$C_E$	$\gamma_I$	$\gamma_B$	$\gamma_P$	$\gamma_A$	$\gamma_n$	$\gamma_T$	$\gamma_R$	$\gamma_\varepsilon$	$\gamma_\kappa$
0.145	0.93	0.15	-0.69	0.19	0.41	0	1.97	0.58	0.78

Now, introducing the normalized quantities

$$\underline{n}=\langle n\rangle/\langle n_0\rangle \quad \underline{T}=\langle T\rangle/\langle T_0\rangle \quad \underline{P}=P/P_r(\langle n_0\rangle, \langle T_0\rangle) \quad \underline{t}=3P_r(\langle n_0\rangle, \langle T_0\rangle)t/W(\langle n_0\rangle, \langle T_0\rangle)$$

the normalized global power balance equation becomes

$$\partial(3\underline{n}\underline{T})/\partial\underline{t}=\underline{n}^2[\Sigma(\langle T_0\rangle, \underline{T})-\underline{T}^{1/2}]+(\underline{T}^{3/2}-\underline{n}^{1-\gamma_n}\underline{T}^{1-\gamma_T}\underline{P}^{\gamma_P}/X+P_{\text{aux}}),$$

where the normalized reactivity  $\Sigma$  is a relatively strong function of  $\underline{T}$ , but weakly dependent of  $\langle T_0\rangle$ , defined by

$$\Sigma(\langle T_0\rangle, \underline{T})=g_\alpha(\langle T_0\rangle)\langle\sigma v\rangle(\langle T_0\rangle)\underline{T}[g_\alpha(\langle T_0\rangle)\langle\sigma v\rangle(\langle T_0\rangle)]^{-1}$$

with  $\Sigma(\langle T_0\rangle, 1)=1$ . If the monomial approximation of the reactivity is used, the  $\Sigma$  function becomes independent of  $\langle T_0\rangle$ :

$$\Sigma(\langle T_0\rangle, \underline{T})\approx\underline{T}^\alpha.$$

In this case, the geometrical and safety factor aspects, plus all the profiles, impurities and neoclassical effects are singly contained in the figure of merit  $X$ . In general, the normalized power balance equation presents an additional weak dependence on the profiles through the reference temperature  $\langle T_0\rangle$  in  $\Sigma$ .

The power balance equation is solved to give the auxiliary power for steady-state operation

$$P_{\text{aux}}=(\underline{n}^{1-\gamma_n}\underline{T}^{1-\gamma_T}/X)^{1/(1+\gamma_P)}-\underline{n}^2[\Sigma(\langle T_0\rangle, \underline{T})-\underline{T}^{1/2}]-\underline{T}^{3/2}.$$

This expression leads to saddle-point geometry (Cordey pass) for the auxiliary power contours in the normalized  $(\underline{T}, \underline{n})$  coordinates. The saddle point position  $(\underline{T}_s, \underline{n}_s)$  is determined solving the equations  $(\partial P_{\text{aux}}/\partial \underline{T})_s=0$  and  $(\partial P_{\text{aux}}/\partial \underline{n})_s=0$ , which give the Cordey pass expression

$$\underline{n}_s = \underline{T}_s^{-1} [3(1-\gamma_n)]^{1/2} \{ (3+\gamma_n-4\gamma_T) - [4(1-\gamma_T) - 2(1-\gamma_n)] d\ln\Sigma/d\ln\underline{T}_s \} \underline{T}_s^{-1/2} \Sigma_s \}^{-1/2}$$

and a transcendental equation relating  $\underline{T}_s$  to  $X$

$$\underline{T}_s^{3(1+\gamma_P)/2 + (\gamma_n - \gamma_T)} (\underline{T}_s^{-1/2} \Sigma_s - 1)^{-(1+\gamma_P)} \{ 1 - (3+\gamma_n-4\gamma_T)^{-1} [4(1-\gamma_T) - 2(1-\gamma_n)] d\ln\Sigma/d\ln\underline{T}_s \} \underline{T}_s^{-1/2} \Sigma_s \}^{(1+\gamma_P) - (1-\gamma_n)/2} \\ = [2(1-\gamma_n)^{-1} (1+\gamma_P)]^{1+\gamma_P} [3(3+\gamma_n-4\gamma_T)^{-1} (1-\gamma_n)]^{(1+\gamma_P) - (1-\gamma_n)/2} X,$$

where  $\Sigma_s = \Sigma(\langle T_0 \rangle, \underline{T}_s)$ .

Additionally taking  $(\underline{P}_{aux})_s = 0$ , one defines the minimal condition for ohmic ignition, that is, the minimum value of  $X = X_i$  that allows a thermal excursion of the plasma from the ohmic ( $\underline{T} < \underline{T}_i$ ) to the ignition ( $\underline{T} > \underline{T}_i$ ) domains. Since the value of  $X$  depends on the machine and plasma parameters, it is possible to search for sets of parameters that satisfy the condition  $X \geq X_i$  and, therefore, imply ohmic ignition capability. In general, the parameter  $X$  measures the tokamak performance, since the ignition margin will be larger for large values of  $X$  even though  $X < X_i$ .

#### 4. Application of the figure of merit concept

Figure 1 shows a sequence of 3D plots of the normalized auxiliary power  $\underline{P}_{aux}$  as a function of the normalized temperature  $\underline{T}$  and density  $\underline{n}$  for the IPB98 scaling law (in the figures the normalized quantities are identified by carets). In the sequence of plots, from left to right, the figure of merit assumes the values  $X=0.823$ ,  $1.059$  and  $1.104$ . The same sequence is shown in Fig. 2, in the form of contour plots.

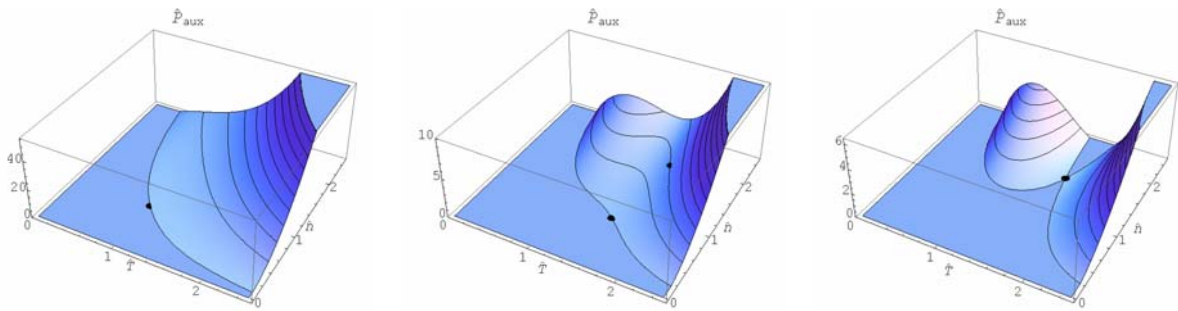


**Fig. 1.** 3D plots of the normalized auxiliary power as a function of the normalized temperature and density. The figure of merit is  $X=0.823$ ,  $1.059$  and  $1.104$ , from left to right. The low point in each plot indicates the transition, on the Cordey pass, from the ohmic to the auxiliary heated domains. The high point in the middle frame indicates a possible ITER-like operating condition for 500 MW of fusion power production.

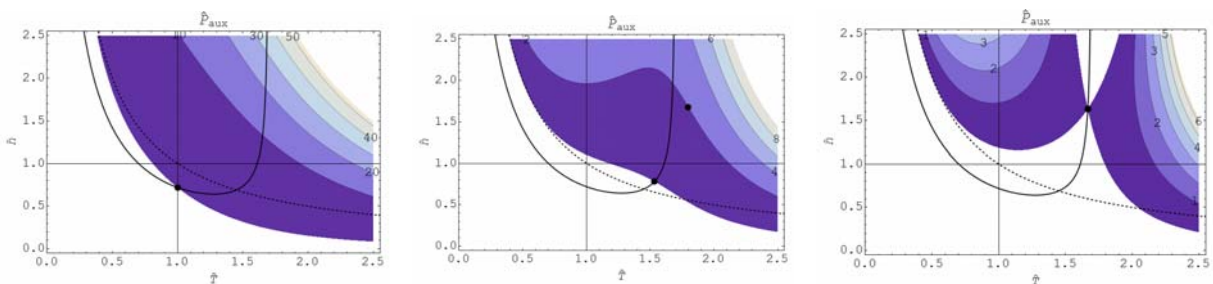


**Fig. 2.** Power contours corresponding to Fig. 1. The vertical line at  $\underline{T}=1$  corresponds to the condition  $P_\alpha = P_r$ , and the dashed line to the condition  $P_Q = P_r$ . The thick line shows the Cordey pass.

The figure of merit  $X=0.823$ , represented in the leftmost frames of Figs. 1 and 2, is interesting because the point of equilibrium  $\underline{P}_{aux}=0$  on the Cordey pass occurs exactly at the reference temperature  $\underline{T}_0=1$ . The middle frames in Figs. 1 and 2 correspond to the figure of merit  $X=1.059$ , calculated for an ITER-like reactor with the reference temperature and density  $\langle T_0 \rangle = 4.92$  keV and  $\langle n_0 \rangle = 0.531 \times 10^{20} \text{ m}^{-3}$ , respectively. The auxiliary power in this case is normalized by the total radiated power  $P_r(\langle T_0 \rangle, \langle n_0 \rangle) = 5.63$  MW, and the point in the upper-right quadrant represents the operational conditions  $\langle T \rangle = 8.85$  keV,  $\langle n \rangle = 0.891 \times 10^{20} \text{ m}^{-3}$ .

and  $P_{aux}=11.2 MW$ , giving  $P_{fusion}=500 MW$  and  $\tau_E=3.7 s$ . Finally, the rightmost frames correspond to the ohmic ignition condition with  $X_i=1.104$ .

The path along the Cordey pass, or saddle point trajectory, gives the conditions for minimum auxiliary power use on the way to ignition. Figure 3 shows, on the left-hand side, the saddle point trajectory in the normalized density versus temperature space for the IPB98 scaling law. For each figure of merit  $X$  there corresponds one saddle point location along the path. On the right-hand side of Fig. 3 it is shown how the temperature and density change along the saddle point trajectory as a function of the figure of merit  $X$ . Ohmic ignition is indicated in both plots of Fig. 3 by the point  $X_i=1.104$ .

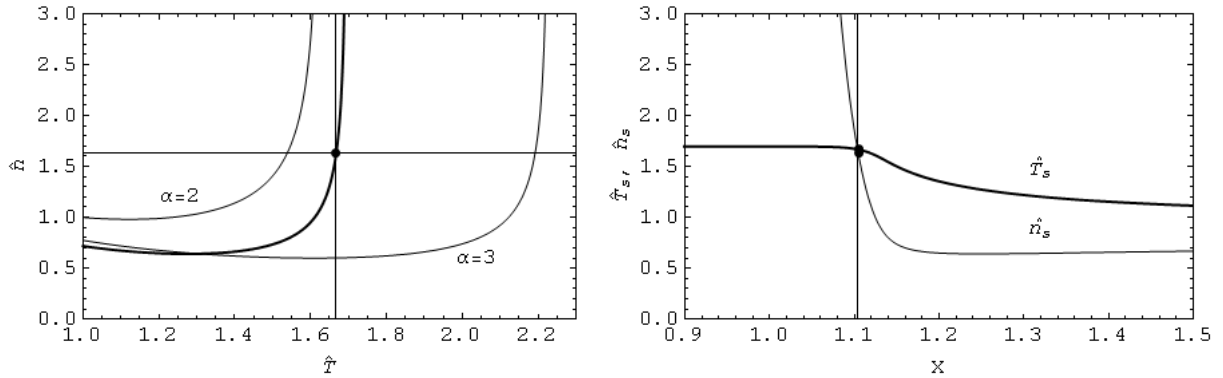


**Fig. 3.** The left-hand side plot shows the saddle point trajectory in the normalized density versus temperature space for the IPB98 scaling law, fixed reference temperature  $\langle T_\theta \rangle = 4.92$  keV, and arbitrary  $X$  value. The point indicates ohmic ignition conditions for  $X=1.104$ . The thick line corresponds to the exact reactivity calculations and the thin lines show the passes obtained using the monomial approximation of the D-T reactivity with  $\alpha=3$  and 2 (a bad approximation in this case). The right-hand side plot displays the saddle point temperature and density as a function of  $X$ . This plot shows that ignition becomes unattainable for the assumed reference temperature and  $X$  less than about 1.08 because of density limits.

The various power contributions can be determined along the favorable Cordey pass for a given scaling law, reference temperature  $\langle T_\theta \rangle$  and value of the figure of merit  $X$ . Actually, the dependence on the reference temperature, which is determined by  $Z_{eff}$ ,  $\alpha_n$ ,  $\alpha_T$  and  $f_a$ , is rather weak for usual cases. Essentially, it is the value of  $X$  that defines the machine performance. Figure 4 shows the normalized alpha, ohmic, radiation and auxiliary power contributions along the pass. Figure 5 shows the fusion gain, normalized fusion power, auxiliary power, and total power deposited on the wall for different operating points along the pass. In both figures the normalized temperature varies from the minimum value  $\underline{T}_s$  which corresponds to  $\underline{P}_{aux}=0$  to the maximum value  $\underline{T}_s=1.696$  where  $\underline{n}_s \rightarrow \infty$ . The sequence in Fig. 4 shows how the performance changes from a driven ITER-like reactor, with  $X=1.059$  and high fusion power output, to an ohmic tokamak with  $X < 0.6$  and relatively low fusion output. For comparison, JET has a figure of merit  $X \sim 0.44$ . Figure 5 illustrates the same transition in performance, emphasizing the fusion gain  $Q$  variation (note the change in the vertical scale).

An examination of the figures, in particular Fig. 5, indicates that a figure of merit  $X=0.6$  or slightly above is adequate for low power reactors, giving  $1 < Q < 3$  with moderate levels of auxiliary heating power. A reactor with  $X \sim 0.4$  (CTF [6] has  $X \sim 0.36$ ) and low values of  $Q$  is also possible, but the plasma will be more like a target for large amounts of auxiliary heating power by neutral beams. Anyway, for nuclear components testing, transmutation and fuel production a strongly driven operation with  $Q < 1$  is acceptable.

Starting from a chosen value of  $X$ , it is possible to search for sets of machine parameters that satisfy the performance goal. For example, consider low-power tokamak reactors with a

figure of merit  $X=0.6$  producing 25 MW of fusion power,  $500 \text{ kW/m}^2$  of wall loading on a close wall and operating along the Cordey pass.

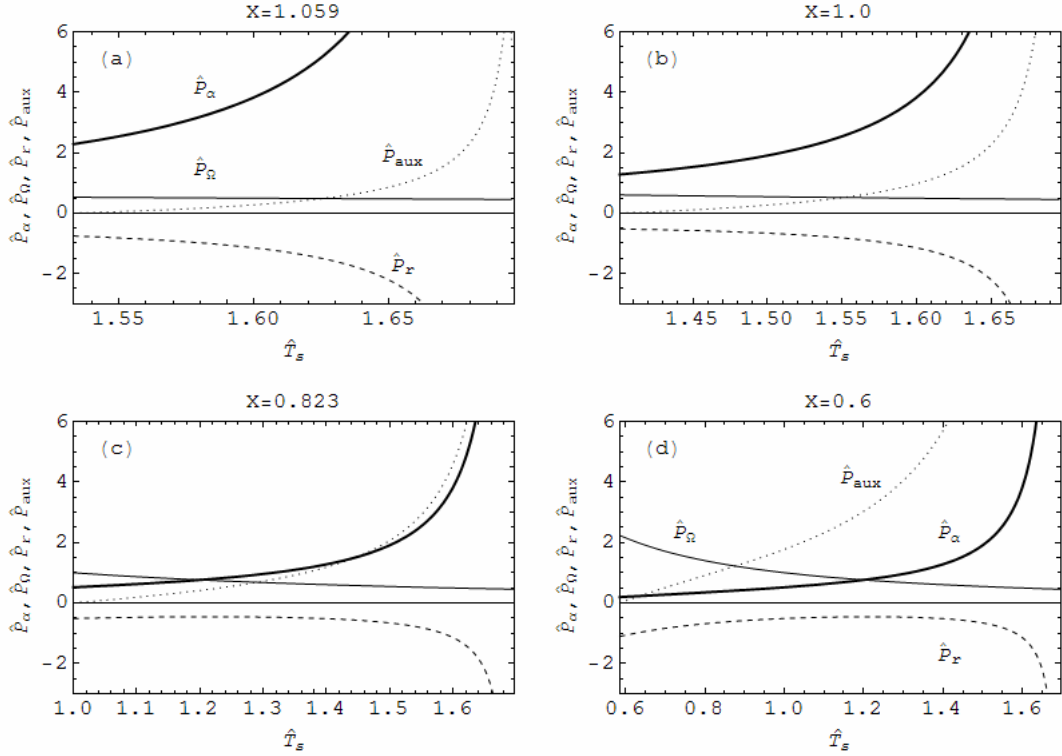


**Fig. 4.** Normalized alpha power (thick line), ohmic power (thin line), radiation power (dashed line), and auxiliary power (dotted line) along the Cordey pass shown in Fig. 3 for fixed reference temperature  $\langle T_0 \rangle = 4.92 \text{ keV}$  and varying figure of merit  $X$ .

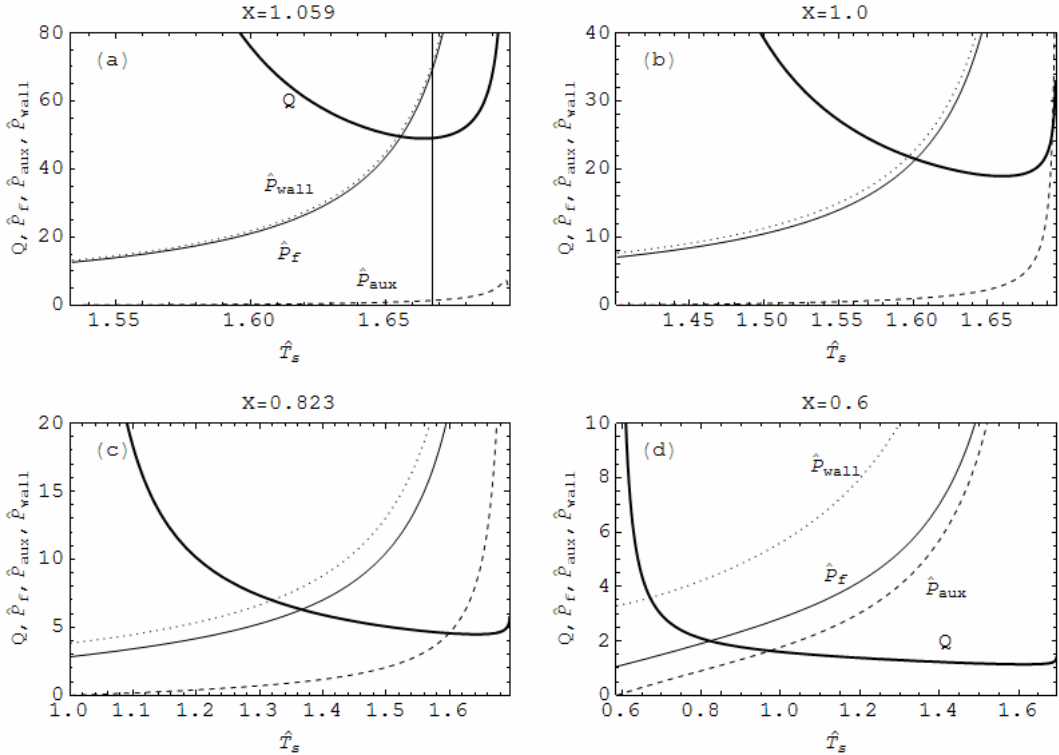


**Fig. 5.** Fusion gain (thick line), fusion power (thin line), auxiliary power (dashed line), and total power deposited on the wall (dotted line) following the saddle point trajectory shown in Fig. 3 for fixed reference temperature  $\langle T_0 \rangle = 4.92 \text{ keV}$  and varying figure of merit  $X$ .

Table 1. Main parameters of possible low-power tokamak reactors.								
A	a (m)	B <sub>0</sub> (T)	I <sub>p</sub> (MA)	q*	T (keV)	n <sub>20</sub> (10 <sup>20</sup> m <sup>-3</sup> )	n <sub>G</sub> (10 <sup>20</sup> m <sup>-3</sup> )	Q
1.6	1.12	2.1	12.7	2.01	3.34	2.79	3.21	2.60
2.0	0.935	3.6	10.0	2.01	5.89	1.33	3.65	1.24

The normalized fusion power is

$$P_f = (E_n/E_\alpha + 1) P_\alpha / f_\alpha$$

and the normalized total power deposited on the wall is given by

$$P_{wall} = (E_n/E_\alpha + 1 - f_\alpha) P_\alpha / f_\alpha + P_c + P_r,$$

where  $E_n = 14.03$  MeV and  $E_\alpha = 3.561$  MeV refer to the energy of the neutrons and alpha particles in the D-T fusion cycle. The close wall surface is simply taken equal to the plasma surface  $A_s$ . Assuming IPB98 scaling law with  $H=1$ , and taking  $\alpha_n=1$ ,  $\alpha_T=1/2$ ,  $\alpha_j=3\alpha_T/2$  (profile consistency),  $Z_{eff}=1.5$ ,  $\kappa=2.5$  and  $\delta=0.4$ , Table 1 lists possible sets of parameters that satisfy the requirements for aspect ratios  $A=1.6$  and  $2.0$ . These results indicate that low-power reactors with minor radius  $a \sim 1$  m, magnetic fields in the 2 to 3 T range and  $1 < Q < 3$  are feasible. With the new scaling laws obtained for low aspect ratio tokamaks [14] similar results can be obtained with about half the plasma current, lower densities and higher temperatures.

**Acknowledgement.** This work was partially supported by the International Atomic Energy Agency under the Co-ordinated Research Project on Joint Research Using Small Tokamaks – IAEA contract No. BRA/12932.

- [1] Wu, Y. *et al* 2006 “Conceptual design of the fusion-driven subcritical system FDS-I” *Fusion Eng. Des.* **81** 1305-1311
- [2] Galvão, R.M.O. *et al* 2008 “Multi-functional Compact Tokamak Reactor Concept” paper FT/P3-20 this conference
- [3] Stacey, W.M. *et al* 2005 “A subcritical, gas-cooled fast transmutation reactor with a fusion neutron source” *Nucl. Technol.* **150** 162-188
- [4] Wu, Y., FDS Team 2006 “Conceptual design activities of FDS series fusion power plants in China” *Fusion Eng. Des.* **81** 2713-2718
- [5] Peng, Y-K.M. *et al* 2005 “A component test facility based on the spherical tokamak” *Plasma Phys. Control. Fusion* **47** B263-B283
- [6] Voss, G. *et al* 2008 “Conceptual design of a component test facility based on the spherical tokamak” *Fusion Eng. Des.* In press
- [7] Tobita, K. *et al* 2007 “SlimCS – compact low aspect ratio DEMO reactor with reduced-size central solenoid” *Nucl. Fusion* **47** 892-899
- [8] Tobita, K. 2008 “A view on DEMO and its superconducting magnet” *First Meeting on the Use of HTS in Tokamaks*, ASIPP, Hefei, Anhui, P.R. China, 20-22 February, 2008
- [9] Gryaznevich, M. 2008 “Use of high temperature superconductors in tokamaks, Introduction” *Ibid*
- [10] Bethe, H.A. 1979 “The fusion hybrid” *Phys. Today*, May 1979
- [11] Ludwig, G.O. and Montes, A. 1990 “Ohmic ignition of small aspect ratio tokamaks”. In *A Variety of Plasmas* (eds.: Sen, A.; Kaw, P.K.), *Proceedings of the 1989 International Conference on Plasma Physics* (New Delhi, 1989) (Bangalore: Indian Academy of Sciences, ISBN-019-562892-6) pp. 489-497
- [12] Wesson, J. 2004 *Tokamaks* (Oxford: Clarendon Press, 2004)
- [13] Uckan, N.A. and Sheffield, J. 1986 “A simple procedure for establishing ignition conditions in tokamaks”. In *Tokamak Startup* (ed. Knoepfel, H.) (New York: Plenum Press, 1986) pp 45-72
- [14] Valovič, M. *et al* 2008 “Confinement and fuelling in MAST” paper EX/P5-17 this conference